Rapid Communications

Dual-frequency spin-resonance spectroscopy of diamond nitrogen-vacancy centers in zero magnetic field

A. K. Dmitriev,[1,*] H. Y. Chen,[2,*] G. D. Fuchs,[2] and A. K. Vershovskii[1,†]
[1]*Ioffe Institute, 194021 St. Petersburg, Russia*
[2]*Cornell University, Ithaca, New York 14853, USA*

(Received 28 February 2019; revised manuscript received 15 May 2019; published 8 July 2019)

The methods for controlling spin states of negatively charged nitrogen-vacancy (NV) centers using microwave (MW) or radio frequency (rf) excitation fields for electron spin and nuclear spin transitions are effective in strong magnetic fields where a level anticrossing (LAC) occurs. A LAC can also occur at zero field in the presence of transverse strain or electric fields in the diamond crystal, leading to mixing of the spin states. In this Rapid Communication, we investigate zero-field LAC of NV centers using dual-frequency excitation spectroscopy. Under rf modulation of the spin states, we observe sideband transitions and Autler-Townes splitting in the optically detected magnetic resonance (ODMR) spectra. Numerical simulations show that the splitting originates from a Landau-Zener transition between electron spin $|\pm1\rangle$ states, which potentially provides a way of manipulating NV center spin states in zero or weak magnetic field.

DOI: 10.1103/PhysRevA.100.011801

Optically detected magnetic resonance (ODMR) in the negatively charged nitrogen-vacancy (NV) center in diamond has been thoroughly studied over the past two decades. Many types of optically detected resonances, both magnetically dependent and magnetically independent, have been investigated, and various methods of controlling both electron and nuclear spins have been developed. These investigations have resulted in the development of high-resolution quantum magnetometers [1–3], as well as methods of frequency stabilization [4]. Resonance techniques for controlling NV center electron and nuclear spins are considered to be highly suitable for quantum information processing because the relaxation time of these spins is long compared to many solid-state quantum objects [5,6]. Typically, either combined microwave (MW) and radiofrequency (rf) excitation [7–14], or electron spin-echo envelope modulation methods [15] are used to address a chosen spin state, allowing for various multiquantum resonances, e.g., as thoroughly studied in Ref. [12]. Various schemes of hole burning using multifrequency MW and rf excitation are discussed in Refs. [14,16]; methods of all-optical excitation ODMR at two frequencies separated by the ground-state zero-field splitting are proposed in Ref. [17].

Multifrequency methods are most effective in strong magnetic fields (0.05 or 0.1 T), where a level anticrossing (LAC) [5,6,12,16,18,19] in either excited or ground states occurs. A LAC between NV center spin states can also occur in weak [19] or zero magnetic fields mediated by external magnetic, intrinsic strain, or electric field transverse to the NV axis. The possibilities of using the zero-field LAC for controlling electron and nuclear spin states, or for exciting narrow resonances for metrological applications are not yet sufficiently explored. Here we present the results of our investigation of the zero-field LAC of NV centers in bulk diamond using dual-frequency (MW + rf) spin resonance spectroscopy. In contrast to normal ODMR spectra, we observe a splitting of the electron spin resonance. The frequency separation of the splitting is identical to the applied rf frequency and independent of magnetic field. When the rf field modulation frequency exceeds the linewidth of spin resonance, sideband transitions arise in the recorded spectra. We numerically simulate the dynamics using a Lindblad master equation and find excellent agreement with our experiment. From the simulation, we note that the splitting in the ODMR spectra originates from strong Landau-Zener transition between the spin $|m_s = +1\rangle$ and $|m_s = -1\rangle$ states mediated by rf modulation and the static intrinsic strain or electric field in diamond. The strongly coupled $\{|m_s = +1\rangle, |m_s = -1\rangle\}$ states, in combination with the spin $|m_s = 0\rangle\}$ state, effectively construct a Δ system, giving rise to the observed splitting from the Autler-Townes (AT) effect. Our approach constitutes a useful way of manipulating NV center spin states in the spin $|m_s = \pm1\rangle$ manifold at zero or low magnetic field.

The spin level structure of the $^3A_2$ ground state of NV centers in external magnetic field is defined by the Hamiltonian [20–22]

$$\begin{aligned} H = {} & D\left(S_z^2 - \tfrac{1}{3}\vec{S}^{\,2}\right) - E_x\left(S_x^2 - S_y^2\right) + E_y(S_xS_y + S_yS_x) \\ & + g_s\mu_B\vec{B}\cdot\vec{S} + A_\parallel S_zI_z + A_\perp(S_xI_x + S_yI_y) \\ & + PI_z^2 - g_I\mu_N\vec{B}\cdot\vec{I}\,, \end{aligned} \tag{1}$$

where $\mu_B = h \times 13.996 \times 10^9$ Hz/T is the Bohr magneton, $\vec{I}$ is the ^{14}N nuclear spin ($I = 1$), $\vec{S}$ is the electron spin of the NV center ($S = 1$), $\mu_N = h \times 7.622 \times 10^6$ Hz/T is the nuclear magneton, $D = (2\pi)2.87$ GHz, and $E = \sqrt{E_x^2 + E_y^2}$ is the transverse zero-field splitting (ZFS) parameters.

*These authors contributed equally to this work.
†antver@mail.ioffe.ru

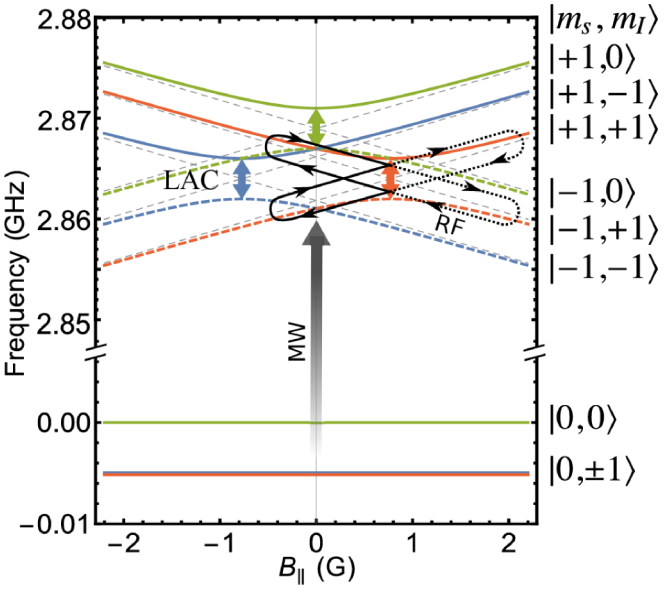

FIG. 1. NV center ground-state splitting frequencies dependence on axial local magnetic field, calculated for a diamond crystal with transverse ZFS parameter $E = (2\pi)2$ MHz. Thin dashed lines represent pure quantum states where $E = 0$. Level anticrossings mediated by transverse strain or electric field are marked by colored arrows. MW-induced spin transitions preserve nuclear spin. The axial component of rf fields can lead to modulation of local magnetic field, $B_\parallel$, and hence a modulation of the spin state energies. Electron spin of an NV center driven through the LAC by the rf field can tunnel into the coupled state via Landau-Zener transition (illustrated by the black paths).

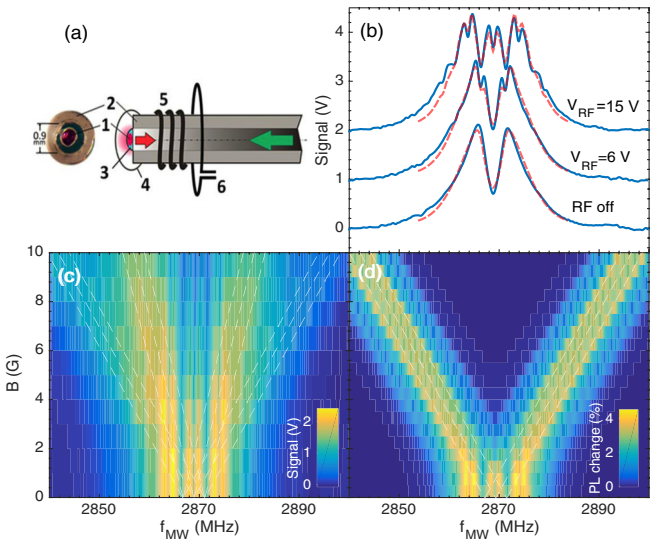

FIG. 2. (a) View of the fiber end, and a schematic diagram of the magnetometer sensor: 1, diamond crystal; 2, optical fiber; 3, transparent glue; 4, reflective coating; 5, MW antenna; 6, rf antenna. (b) ODMR spectra of NV centers taken with gradually increasing rf field amplitude at $f_{rf} = 5$ MHz [1 V corresponds to $(2\pi)0.23(3)$ MHz in terms of Rabi frequency of rf field]. Red dashed lines are a fit from numerical simulation. (c) ODMR spectra recorded at external field B=(0 to 1) mT along the (1,1,1) crystal axis with additional rf excitation at $f_{rf} = 5$ MHz, rf amplitude 15 V. Spin transitions with a larger Zeeman splitting correspond to the axially aligned NV centers. (d) Numerical simulated results for NV centers oriented along the (1,1,1) direction in (c). White dashed lines are guidelines for hyperfine spin transitions.

Depending on the local crystal strain and electric field, E ranges from 0 for an unstressed diamond to up to more than $(2\pi)10$ MHz in highly strained diamond. $g_s = 2.003$ and $g_I = 0.403$ are electron and nuclear g factors, $A_\parallel = -(2\pi)2.16$ MHz and $A_\perp = -(2\pi)2.7$ MHz are axial and transverse hyperfine splitting parameters, and $P = -(2\pi)4.95$ MHz is the quadrupole splitting parameter. We denote eigenstates of the ground state $|m_s, m_I\rangle$; for NV centers with the nitrogen isotope ^{14}N, both electronic and nuclear spin projections take values $m_s, m_I = 0, \pm1$.

The energy structure of NV centers in zero and weak magnetic fields is more complex than in strong ones (Fig. 1); it contains both level crossings and anticrossings. Depending on the strength of the field inhomogeneity, the crossings and level anticrossings may be partially masked by the inhomogeneity of the crystal's internal fields. Each NV center in a bulk sample is affected by local magnetic and electric or strain fields. At $B \approx 0$, the transverse component of the electric or strain field causes $|m_s = \pm1\rangle$ states to mix into superposition states, and transverse magnetic fields cause a second-order LAC [19]. The dependence of the energy levels and corresponding frequencies on magnetic field, B, in the low-field regime is substantially nonlinear. This structure was investigated in detail in [19].

The experiment was conducted at the Ioffe institute. The experimental setup has been described in [23]: a synthetic diamond of SDB1085 60/70 grade (manufactured by Element Six, processed at the Lebedev Physical Institute) with dimensions $0.1 \times 0.3 \times 0.3$ mm is subjected to electron irradiation (5×10^{18} cm^{-2}) and subsequent annealing in Ar at 800 °C for 2 h. Using an optically transparent glue, we then fix the diamond crystal to the end of an optical fiber with a core diameter of 0.9 mm; the wide fiber aperture ensures effective collection of the photoluminescence (PL) signal at the cost of losing ∼90% of pumping light. We increase the pumping and detection efficiency by covering the outer surfaces of the diamond and the end of the optical fiber with a nonconductive reflective coating [Fig. 2(a)].

We focus the pumping beam (∼15 mW at a wavelength of 532 nm) at the second end of the fiber, and collect the PL signal from the same end. Given an overall pumping efficiency of $< 10\%$, the pumping power was far below the optimum [10]. We perform dual-frequency spectroscopy by exciting ODMR in B=(0 to 1) mT using a MW drive field f_{MW} in combination with an additional rf field f_{rf}. We use low-frequency amplitude modulation of the MW field and synchronous detection at the modulation frequency in order to subtract the fluorescence background. All the experiments are done at room temperature.

Without the rf field, the normal ODMR spectra [Fig. 2(b)] appears with two broad peaks in zero magnetic field. The splitting between the two peaks can be attributed to transverse static strain or electric field, E, intrinsic to the diamond [24]. After fitting to a simulated ODMR spectrum, we find an inhomogeneity in the range $E = 0$ to $(2\pi)15$ MHz for the NV

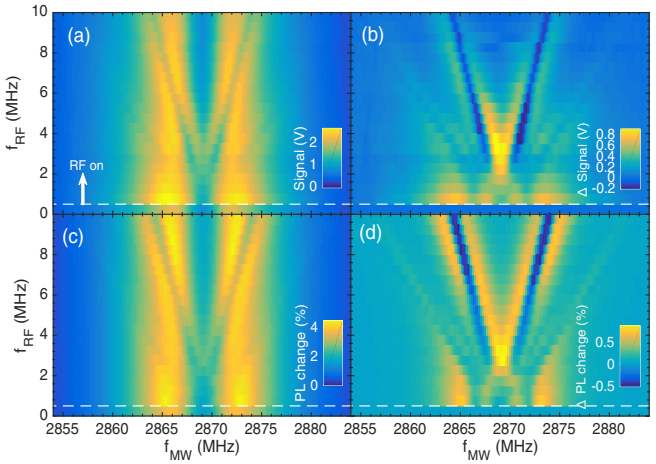

FIG. 3. (a) ODMR spectra recorded at zero external field at different radio frequencies $f_{\rm rf}$ and a fixed amplitude of 6 V [1 V corresponds to $(2\pi)0.23(3)$ MHz in terms of Rabi frequency]; the lowest row at zero frequency is the ODMR signal without rf driving. Splitting occurs in the ODMR spectra when the rf field is applied, with a separation equal to the applied rf frequency. (b) Figure (a) subtracted from the normal ODMR spectrum when the rf is off. First-order and second-order sideband spin transitions are present. (c) and (d) are numerical simulations of the experiment, which agree well with the data.

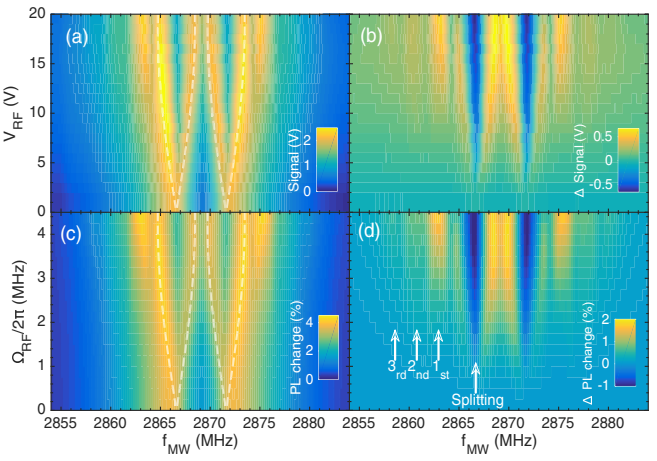

FIG. 4. (a) ODMR spectra taken with an increasing rf field amplitude at a fixed frequency, $f_{\rm rf} = 5$ MHz. (b) Figure (a) subtracted from the ODMR spectrum when rf is off. Sideband transitions up to third order are present. (c) and (d) are numerical simulations of the experiment. Overlay white dashed lines are theoretical predictions of the splitting from Eq. (3), assuming $E = (2\pi)2$ MHz.

center ensemble in our sample, with an approximate Gaussian probability distribution, $p(E) = \frac{1}{\sqrt{2\pi}\sigma} \exp(-E^2/2\sigma^2)$, where $\sigma = (2\pi)5$ MHz. We then apply a rf field with gradually increasing amplitude and a fixed frequency, $f_{\rm rf} = 5$ MHz. The recorded ODMR spectrum [Fig. 2(b)] splits in each broad peak at f_{s+} and f_{s-}, and the separation of the splitting is equal to the applied rf field frequency [25], and is symmetrical about the zero field splitting: $f_{s+} - f_{s-} = f_{\rm rf}$, $(f_{s+} + f_{s-})/2 = D$. Comparing to the normal ODMR spectrum, there are increases in signal amplitude, both in between and outside the splitting in the rf dressed ODMR spectrum. They are around 5 MHz apart with respect to the peaks of the normal ODMR spectrum, which are later associated with the first- and second-order sideband spin resonance transitions.

To interrogate the origin of the observed features, we then carry out experiments at both zero and weak (<1 mT) magnetic field. We first investigate possible magnetic field dependence of the observed splitting, we apply an external magnetic field [along the (111) direction of the diamond lattice; Fig. 2(c)], $B = (0$ to $1)$ mT, and record ODMR spectra with the same rf driving field. As B increases, the splitting gradually fades while the separation of the splitting remains equal to the applied rf field frequency, independent of B. In a sufficiently strong B field, spin resonances of two groups (the group with the larger splitting corresponds to the aligned NV centers) of NV centers appear due to the Zeeman effect. Each electron spin transition contains three peaks, corresponding to the hyperfine hybridization by ^{14}N nuclear spin.

After excluding the effect of the magnetic field, we focus on the study in zero field. With fixed rf driving amplitude, we vary the applied rf field frequency from 0.5 to 10 MHz. The resulting ODMR spectra are plotted in Fig. 3. To emphasize the effect of rf driving, in Fig. 3(b), we subtract the spectra in Fig. 3(a) by the normal ODMR spectra without a rf field. The differences in the rf dressed ODMR spectra reveal the following: (1) the splitting occurs for the entire rf frequency range (0.5–10 MHz) in a V shape, with a separation that grows linearly with the applied rf frequency; (2) sideband transitions are apparent outside the splitting as a result of spin level modulation of the rf field; (3) a LAC is observed in between first-order and second-order sidebands.

In the third experiment, we keep the rf frequency fixed at 5 MHz, and record ODMR spectra with increasing rf field amplitude (Fig. 4). We observe the splitting grows first linearly and then sublinearly as the applied rf field amplitude increases. Sideband transitions up to the third order are present in the probed range.

To interpret the experimental results, we ran numerical simulations using a 19×19 Hamiltonian comprising nine hyperfine levels in the ground states, nine hyperfine levels in the excited states, and a singlet level that is accessed via the intersystem crossing. We initialize the density matrix of the system in an unpolarized ground spin state, and evolve the system using a Lindblad master equation. Fluorescence of NV centers are calculated through the population in nine excited hyperfine states that decay directly into the corresponding ground states, preserving electron or nuclear spin. Considering the inhomogeneity of the strain (or electric field) in our sample, we simulate dual-frequency ODMR spectra for NV centers of various strain, $E = 0$ to $(2\pi)15$ MHz, and average the spectra with a normal distribution of the strain $p(E)$. Using the parameters MW probe field Rabi frequency $(2\pi)0.5$ MHz and laser excitation optical Rabi frequency $(2\pi)2$ MHz, the simulated results are in excellent agreement with experimental data [Figs. 3(c) and 3(d) and Figs. 4(c) and 4(d)].

We now unravel the mechanism of splitting and sideband transitions in our experiment. For simplicity, we restrict the discussion to the $\{|-1,+1\rangle,\ |+1,+1\rangle\}$ basis for a single

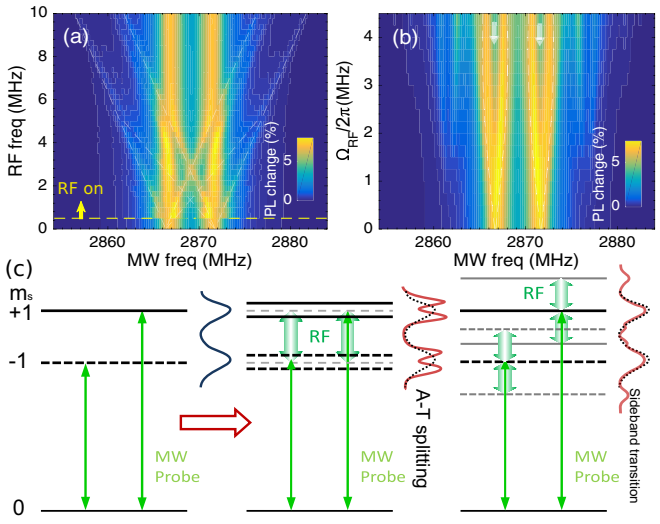

FIG. 5. Numerically simulated dual-frequency ODMR spectra for a single NV center with transverse strain $E = (2\pi)1.5$ MHz. The rf driving field is kept at $\Omega_{\rm rf} = (2\pi)2$ MHz in (a) and $f_{\rm rf} = 5$ MHz in (b). White dashed lines in (a) and arrows in (b) are guidelines for sideband transitions and AT splitting, respectively. (c) Level diagrams of rf dressed spin states, showing effects of AT splitting and sideband transitions.

NV center. Figure 5 shows the numerically simulated dual-frequency ODMR spectra for a single NV center with transverse strain $E = (2\pi)2$ MHz. In the rotating frame of the MW field and in the absence of an external magnetic field, the Hamiltonian of the above states can be written as

$$H = \begin{pmatrix} -A_\parallel + \Omega_{\rm rf}\cos(2\pi f_{\rm rf}t) & E \\ E & A_\parallel - \Omega_{\rm rf}\cos(2\pi f_{\rm rf}t) \end{pmatrix}, \quad (2)$$

where $\Omega_{\rm rf}$ and $f_{\rm rf}$ are the amplitude and frequency of the rf driving field. The two levels are coupled by a transverse strain field, E. The rf magnetic field modulates the energy of the two levels through the longitudinal Zeeman coupling. When $\Omega_{\rm rf} - A_\parallel > E$, as the two levels approach each other diabatically, transitions can occur through Landau-Zener tunneling (LZT) [26] with a probability around $1 - e^{-E^2/f_{\rm rf}\Omega_{\rm rf}}$, as demonstrated in [18,27] for a single NV center between $|+1, 0\rangle$ and $|0, 0\rangle$ states at finite field. In our experiment, the NV ensemble in the sample has transverse coupling field E ranging from 0 to $(2\pi)15$ MHz and averaging around $(2\pi)2$ MHz. For the rf driving field with $\Omega_{\rm rf} > A_\parallel$ and $2\pi f_{\rm rf} > E$, the diabaticity requirement is always met for some of the NV centers in the ensemble. Therefore, the LZT mechanism applies for most of the range probed in our experiment and for rf fields beyond the power and frequency used here. A detailed study of the Hamiltonian in Eq. (2) can be found in Refs. [28,29]. To explain the splitting, we apply the polaron transformation, such that the effective Hamiltonian becomes [28,30]

$$H' = \begin{pmatrix} -2\pi f_{\rm rf} + \Delta & \widetilde{\Omega}^\dagger \\ \widetilde{\Omega} & -\Delta \end{pmatrix},$$

$$\widetilde{\Omega} = -\Omega_{\rm rf}\sin 2\theta \sum_n J_n\left(2\frac{\Omega_{\rm rf}}{2\pi f_{\rm rf}}\cos 2\theta\right)e^{in2\pi f_{\rm rf}t}, \quad (3)$$

where $\tan 2\theta = -E/A_\parallel$, $\Delta^2 = A_\parallel^2 + E^2$. J_n is the Bessel function of the first kind. When the rf field frequency meets the condition $2\pi f_{\rm rf} = 2\Delta$, a LZT spin transition occurs. When the rf driving amplitude is strong enough, the system is well described by a dressed-states picture in which the rf field introduces a splitting $2\widetilde{\Omega}$ in the ODMR spectra (white dashed line trace in Fig. 4). Taking into account the spin $|m_s = 0\rangle$ state, we have a three-level system, with spin $|m_s = \pm 1\rangle$ states coupled via transverse strain and rf field, probed by the MW transition from the spin $|m_s = 0\rangle$ state. In the strongly driven regime, this constitutes an Autler-Townes type structure. Due to rf field longitudinal level modulation of spin states, sideband transitions also occur in our spectra, which has been reported in [12]. Applying the rotating frame and rotating wave approximation [29] (or Floquet theory [31]), H becomes

$$H_{\rm RWA} = \begin{pmatrix} -A_\parallel & EJ_n\left(\frac{\Omega_{\rm rf}}{2\pi f_{\rm rf}}\right) \\ EJ_n\left(\frac{\Omega_{\rm rf}}{2\pi f_{\rm rf}}\right) & A_\parallel - 2n\pi f_{\rm rf} \end{pmatrix}. \quad (4)$$

Sideband transitions of nth order arise at $nf_{\rm rf}$ away from the unperturbed transition frequency.

We exclude other origins for the splitting seen in the experiment; for instance, a transverse magnetic field from stray or earth field, rf driving of nuclear spin transitions, because the transverse magnetic field only induces mixing between $|\pm 1, m_I\rangle$ and $|0, m_I\rangle$ states, and nuclear spin flops driven by the rf field occur only within states of the same electron spin. Neither is able to drive a transition between the $|-1, m_I\rangle$ and $|+1, m_I\rangle$ states.

Note that transitions between the $|-1, m_I\rangle$ and $|+1, m_I\rangle$ states of an NV center are magnetically forbidden; however, our results show that such transitions can be driven through LZT using a rf field for a strained NV center in zero or weak magnetic field. Future experiments that implement pulsed MW and rf sequences could be used to coherently control the spin states for the $|m_s = \pm 1\rangle$ levels through LZT at low field. Specifically, after initializing the NV center spin in the $|-1, m_I\rangle$ or the $|+1, m_I\rangle$ state, coherent Rabi oscillations at $2\widetilde{\Omega}$ could be observed by recording the time evolution of the spin population when a rf field of amplitude $\Omega_{\rm rf} > A_\parallel$ and frequency $2\pi f_{\rm rf} = 2\Delta$ is turned on. Similar protocols have been both theoretically established [28] and experimentally demonstrated [18]. Given that strain and electric fields are prevalent in diamond crystals, rf control of spin $|m_s = \pm 1\rangle$ states can be readily applied to a single NV center.

In conclusion, we perform dual-frequency spin resonance spectroscopy on NV centers using MW and rf fields in zero or weak magnetic field, and report the detection of Autler-Townes splitting and sideband transitions in the recorded ODMR spectra. Numerical simulations reveal that the splitting is caused by strong Landau-Zener tunneling between $|-1, m_I\rangle$ and $|+1, m_I\rangle$ states, mediated by a zero-field LAC due to the transverse strain or electric field. This is a normally forbidden magnetic transition, thus demonstrating an alternative mechanism for manipulating NV center ground spin states.

Research support at Cornell University was provided by the Office of Naval Research (Grant No. N000141712290).

[1] J. M. Taylor, P. Cappellaro, L. Childress, L. Jiang, D. Budker, P. R. Hemmer, A. Yacoby, R. Walsworth, and M. D. Lukin, Nat. Phys. **4**, 810 (2008).

[2] G. Balasubramanian, I. Y. Chan, R. Kolesov, M. Al-Hmoud, J. Tisler, C. Shin, C. Kim, A. Wojcik, P. R. Hemmer, A. Krueger, T. Hanke, A. Leitenstorfer, R. Bratschitsch, F. Jelezko, and J. Wrachtrup, Nature (London) **455**, 648 (2008).

[3] V. M. Acosta, E. Bauch, A. Jarmola, L. J. Zipp, M. P. Ledbetter, and D. Budker, Appl. Phys. Lett. **97**, 174104 (2010).

[4] J. S. Hodges, N. Y. Yao, D. Maclaurin, C. Rastogi, M. D. Lukin, and D. Englund, Phys. Rev. A **87**, 032118 (2013).

[5] F. Jelezko, T. Gaebel, I. Popa, M. Domhan, A. Gruber, and J. Wrachtrup, Phys. Rev. Lett. **93**, 130501 (2004).

[6] V. Jacques, P. Neumann, J. Beck, M. Markham, D. Twitchen, J. Meijer, F. Kaiser, G. Balasubramanian, F. Jelezko, and J. Wrachtrup, Phys. Rev. Lett. **102**, 057403 (2009).

[7] M. V. G. Dutt, L. Childress, L. Jiang, E. Togan, J. Maze, F. Jelezko, A. S. Zibrov, P. R. Hemmer, and M. D. Lukin, Science **316**, 1312 (2007).

[8] P. Neumann, N. Mizuochi, F. Rempp, P. Hemmer, H. Watanabe, S. Yamasaki, V. Jacques, T. Gaebel, F. Jelezko, and J. Wrachtrup, Science **320**, 1326 (2008).

[9] L. Jiang, J. S. Hodges, J. R. Maze, P. Maurer, J. M. Taylor, D. G. Cory, P. R. Hemmer, R. L. Walsworth, A. Yacoby, A. S. Zibrov, and M. D. Lukin, Science **326**, 267 (2009).

[10] B. Smeltzer, J. McIntyre, and L. Childress, Phys. Rev. A **80**, 050302(R) (2009).

[11] M. Steiner, P. Neumann, J. Beck, F. Jelezko, and J. Wrachtrup, Phys. Rev. B **81**, 035205 (2010).

[12] L. Childress and J. McIntyre, Phys. Rev. A **82**, 033839 (2010).

[13] C. Wei and N. B. Manson, J. Opt. B: Quantum Semiclassical Opt. **1**, 464 (1999).

[14] N. B. Manson, L. J. Rogers, E. A. Wilson, and C. Wei, J. Lumin. **130**, 1659 (2010).

[15] E. V. Oort and M. Glasbeek, Chem. Phys. **143**, 131 (1990).

[16] P. Kehayias, M. Mrozek, V. M. Acosta, A. Jarmola, D. S. Rudnicki, R. Folman, W. Gawlik, and D. Budker, Phys. Rev. B **89**, 245202 (2014).

[17] V. M. Acosta, K. Jensen, C. Santori, D. Budker, and R. G. Beausoleil, Phys. Rev. Lett. **110**, 213605 (2013).

[18] G. D. Fuchs, G. Burkard, P. V. Klimov, and D. D. Awschalom, Nat. Phys. **7**, 789 (2011).

[19] H. Clevenson, E. H. Chen, F. Dolde, C. Teale, D. Englund, and D. Braje, Phys. Rev. A **94**, 021401(R) (2016).

[20] S. Felton, A. M. Edmonds, M. E. Newton, P. M. Martineau, D. Fisher, D. J. Twitchen, and J. M. Baker, Phys. Rev. B **79**, 075203 (2009).

[21] R. Fischer, A. Jarmola, P. Kehayias, and D. Budker, Phys. Rev. B **87**, 125207 (2013).

[22] M. W. Doherty, F. Dolde, H. Fedder, F. Jelezko, J. Wrachtrup, N. B. Manson, and L. C. L. Hollenberg, Phys. Rev. B **85**, 205203 (2012).

[23] A. K. Dmitriev and A. K. Vershovskii, J. Opt. Soc. Am. B **33**, B1 (2016).

[24] T. Mittiga, S. Hsieh, C. Zu, B. Kobrin, F. Machado, P. Bhattacharyya, N. Z. Rui, A. Jarmola, S. Choi, D. Budker, and N. Y. Yao, Phys. Rev. Lett. **121**, 246402 (2018).

[25] A. K. Dmitriev and A. K. Vershovskii, J. Phys.: Conf. Ser. **1135**, 012051 (2018).

[26] L. D. Landau, Phys. Z. Sowjetunion **1**, 88 (1932); C. Zener, Proc. R. Soc. London, Ser. A **137**, 696 (1932); E. C. G. Stückelberg, Helv. Phys. Acta **5**, 369 (1932).

[27] P. Huang, J. Zhou, F. Fang, X. Kong, X. Xu, C. Ju, and J. Du, Phys. Rev. X **1**, 011003 (2011).

[28] S. Ashhab, J. R. Johansson, A. M. Zagoskin, and F. Nori, Phys. Rev. A **75**, 063414 (2007).

[29] W. D. Oliver, Y. Yu, J. C. Lee, K. K. Berggren, L. S. Levitov, and T. P. Orlando, Science **310**, 1653 (2005).

[30] H. Y. Chen, E. R. MacQuarrie, and G. D. Fuchs, Phys. Rev. Lett. **120**, 167401 (2018).

[31] S. K. Son, S. Han, and Shih-I. Chu, Phys. Rev. A **79**, 032301 (2009).